



Structure of the Benzene Dimer—Governed by Dynamics**

Melanie Schnell,* Undine Erlekam, P. R. Bunker, Gert von Helden, Jens-Uwe Grabow, Gerard Meijer, and Ad van der Avoird*

The benzene dimer is a prototypical system for studying noncovalent interactions between aromatic systems. It exhibits two competing equilibrium structures, a tilted T-shaped one (edge-to-face arrangement) and a parallel-displaced one (stacked arrangement). Both the subtle difference in the binding energies of the two structures and the complex internal dynamics of the dimer are particularly challenging and have received much attention from experimentalists and theoreticians. This is, for example, summarized in Ref. [1]. Such competing arrangements of aromatic fragments also play an important role in the structure and dynamic behavior of proteins and DNA.

The first (1975) experimental study of the benzene dimer formed in a molecular beam^[2] determined that it is polar, which suggests that its structure is T-shaped. In 1992 Henson et al. demonstrated in their Raman spectroscopic study^[3] that in the benzene dimer there are two inequivalent monomer sites, one of low and one of higher symmetry. Their experimental findings are consistent with a T-shaped equilibrium geometry in which the benzene moiety at the top of the T, in other words the cap, is freely rotating about its C_6 axis. In 1993 Arunan and Gutowsky recorded the rotational spectrum of the benzene dimer using Fourier transform microwave (FTMW) spectroscopy.^[4] Surprisingly, they observed the rotational spectrum of a prolate symmetric rotor with rich substructure that was tentatively assigned to two independent internal motions, such as two opposed interconversion pathways. However, neither the unexpected symmetric-rotor spectrum nor the substructure have been explained to date.

In ab initio electronic structure theory, the benzene dimer is often used as a benchmark system for calculating dispersion forces between nonpolar molecules. Recent theoretical studies agree that the tilted T-shaped structure is the global

minimum, only 0.43 kJ mol^{-1} (36 cm^{-1}) lower in energy than the nonpolar parallel-displaced one.^[1,6] An ab initio global six-dimensional intermolecular potential surface has been developed for the benzene dimer.^[1,6] Several possible tunneling pathways hindered by only low barriers have been identified, indicating the rich internal dynamics of this floppy system. The three tunneling motions of the benzene dimer that play the main role in this paper are displayed in Figure 1. Tunneling motions can lead to characteristic line splittings in the rotational spectrum. Their analysis allows for a precise determination of the corresponding tunneling mechanisms and the barriers involved. Meanwhile, the experimental observations and ab initio calculations agree on the global minimum structure, the tilted T-shaped structure, but the dynamics of the benzene dimer are still not understood. The present work aims at closing this knowledge gap by employing a combined high-resolution FTMW spectroscopic and theoretical study of the benzene dimer (C_6H_6)₂ and its mixed isotopologue (C_6D_6)^C(C_6H_6)^S with C_6D_6 in the cap and C_6H_6 in the stem of the T-shaped structure, supported by Stark shift measurements to determine its dipole moment.

In agreement with the findings of Arunan and Gutowsky,^[4] we observed the rotational spectrum of a prolate symmetric rotor, although the tilted T-shaped structure was predicted to exhibit the spectrum of a near-prolate asymmetric rotor. Note that the parallel-displaced structure, which is the second energetically low-lying minimum, is nonpolar and thus not visible for FTMW spectroscopy. We recorded 16 rotational transitions belonging to the symmetric-rotor spectrum, ranging from $J+1, K \leftarrow J, K = 4, 1 \leftarrow 3, 1$ at 3413.6 MHz to $10, 2 \leftarrow 9, 2$ at 8476.5 MHz. Figure 2A displays the $6, 0 \leftarrow 5, 0$ transition as an example of a typical symmetric-rotor transition in (C_6H_6)₂. Each transition is split into four

[*] Dr. M. Schnell
Center for Free-Electron Laser Science
Luruper Chaussee 149, 22761 Hamburg (Germany)

Dr. M. Schnell
Max-Planck-Institut für Kernphysik
Saupfercheckweg 1, 69117 Heidelberg (Germany)
E-mail: melanie.schnell@asg.mpg.de

Dr. U. Erlekam, Dr. P. R. Bunker, Dr. G. von Helden,
Prof. Dr. G. Meijer, Prof. Dr. A. van der Avoird
Fritz-Haber-Institut der Max-Planck-Gesellschaft
Faradayweg 4–6, 14195 Berlin (Germany)

Dr. P. R. Bunker
National Research Council of Canada, Ottawa (Canada)

Prof. Dr. J.-U. Grabow
Institut für Physikalische Chemie und Elektrochemie, Gottfried
Wilhelm Leibniz Universität Hannover
Callinstrasse 3a, 30167 Hannover (Germany)

Prof. Dr. A. van der Avoird
Theoretical Chemistry, Institute for Molecules and Materials,
Radboud University Nijmegen
Heyendaalseweg 135, 6525 AJ Nijmegen (The Netherlands)
E-mail: A.vanderAvoird@theochem.ru.nl

[**] We thank Gerrit Groenenboom for useful discussions. This research was supported by the Fonds der Chemischen Industrie (Dozentenstipendium to M.S.), the Alexander von Humboldt Foundation (Humboldt Senior Research Award to A.v.d.A.), the Deutsche Forschungsgemeinschaft (J.-U.G., M.S.), and the excellence cluster "The Hamburg Centre for Ultrafast Imaging" (M.S.). P.R.B. thanks the Fritz-Haber-Institut for continuing hospitality.

Supporting information for this article is available on the WWW under <http://dx.doi.org/10.1002/anie.201300653>.

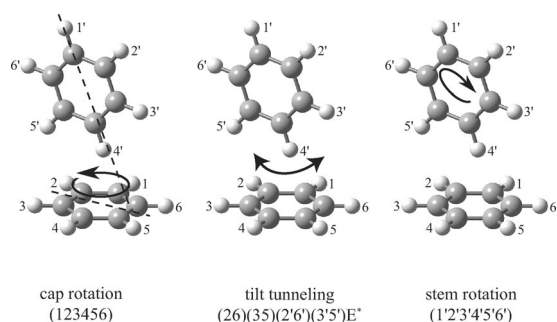


Figure 1. Tilted T-shaped equilibrium structure of the benzene dimer. The bonded carbon–hydrogen units are numbered 1–6 for the cap and 1'–6' for the stem. The stem plane bisects the cap between 2,1,6 and 3,4,5 with 4' pointing at the bond connecting units 5 and 6. This is referred to as the C_s over bond structure. The three tunneling motions in the benzene dimer relevant in this paper are depicted by arrows and as nuclear permutations. These permutations and inversion E^* are elements of the full molecular (or permutation-inversion) symmetry group C_{576} of the benzene dimer.^[1,5] The corresponding barrier heights increase from left to right.

components with an intensity ratio of 3:2:2:1 (starting from the lower-frequency end). The actual transition frequency of each component is the arithmetic mean of a pair of Doppler split peaks shown in Figure 2A. The splittings between consecutive lines in each quartet show the same characteristic 1:2:1 ratio. Note that these $\Delta J=1$ transitions obey the selection rules illustrated in Figure 2B, so the observed splittings reflect the *change* of the tunneling splitting in the levels for subsequent rotational quantum numbers J . As shown in Figure 2B, the different stem sixfold rotation tunneling levels are labeled by the quantum number $k_{\text{stem}} = 0, \pm 1, \pm 2, 3$, with the ± 1 and ± 2 levels being doubly degenerate.

We could individually fit each component of the quartet to a semirigid symmetric-rotor Hamiltonian including centrifugal distortion. This is a strong indication that the internal dynamics can be treated within the high-barrier limit.^[7] The transitions are listed in Table I of the Supporting Information, along with the residuals from individual fits using the symmetric-rotor Hamiltonian. The fitting results are summarized in Table II of the Supporting Information. The obtained rotational constant B ranges from 427.7277(2) MHz for the low-frequency components to 427.7479(3) MHz for the high-frequency components and thus nicely agrees with the value of $(B+C)/2 = 430.0$ MHz calculated for the T-shaped structure (see Table 9 of Ref. [1], rotational constants $A = 1914.5$ MHz, $B = 445.75$ MHz, $C = 414.25$ MHz). For the nonpolar parallel-displaced isomer the calculated value of $(B+C)/2$ is 626.7 MHz.

To shed more light onto the corresponding tunneling pathways, we also measured the rotational spectrum of a partially deuterated isotopologue. Only $(C_6D_6)^C(C_6H_6)^S$, the dimer with the fully deuterated benzene moiety in the cap, was investigated, since the mixed dimer with C_6D_6 in the stem is not present in the molecular beam.^[8] We detected eight rotational transitions again of a prolate symmetric rotor with an effective B rotational constant of 409 MHz. The results are

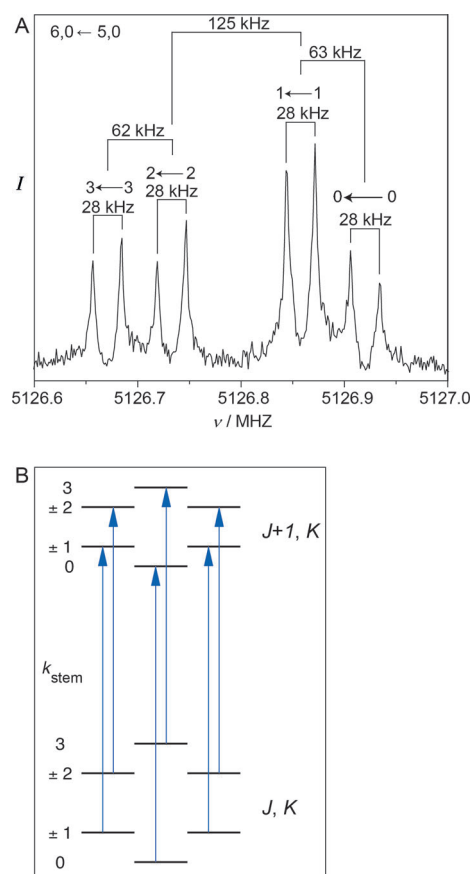


Figure 2. A) Typical symmetric-rotor $J+1, K \leftarrow J, K = 6, 0 \leftarrow 5, 0$ transition of $(C_6H_6)_2$ measured with neon as the carrier gas. Each component is split (here by 28 kHz, as indicated with bars) due to the Doppler effect typical for the coaxially oriented beam resonator arrangement (COBRA) FTMW spectrometer. Above each component it is indicated to which k_{stem} transition this line is assigned (see Figure 2B). For reasons explained in the Supporting Information the intensities displayed here do not reflect the actual 3:2:2:1 intensity ratio. B) Allowed $\Delta J=1, \Delta K=0$ transitions; the quantum numbers k_{stem} correspond to the different stem-rotation tunneling levels of the lower and upper rotational states.

listed in Tables III and IV of the Supporting Information. Again a characteristic quartet pattern with a 1:2:1 line splitting ratio was observed, but due to additional nuclear quadrupole hyperfine structure originating from the six deuterium nuclei (with spin $I_D = 1$) the lines are broader and the peak intensities are lower. No attempt was undertaken to accurately determine the relative intensities of the four tunneling components in this case. The tunneling splitting observed for $(C_6D_6)^C(C_6H_6)^S$ is reduced by as much as 30% compared to the $(C_6H_6)_2$ splittings.

The vibration-rotation-tunneling (VRT) states of the benzene dimer have been calculated^[1] on a six-dimensional ab initio intermolecular potential surface. It was found indeed that the structures corresponding to the low-lying VRT states are essentially T-shaped, that the benzene molecule in the cap rotates almost freely, and that another internal motion occurs: so-called “tilt tunneling”. The line splittings observed in the microwave spectra could not be explained, however. Also in calculations with a one-dimensional (1D) model for the

hindered rotation of the stem^[1,9] these splittings could not be understood. To unravel the mechanism behind the observed splittings, we developed a reduced-dimensionality approach built on a two-dimensional cut of the six-dimensional *ab initio* potential energy surface used in our previous theoretical study of the benzene dimer.^[1] Three of the internal angles are frozen at their equilibrium values in this approach, and also the distance *R* between the monomers' centers of mass is fixed. The two internal motions considered in the model are hindered rotation of the stem and tilt tunneling (see Figure 1), coupled both by the intermolecular potential and by an angular momentum coupling term in the kinetic energy operator. Also the overall rotation of the dimer and Coriolis coupling with the internal rotations is included in the model. More details of our theoretical approach are given in the Supporting Information; the complete theoretical background will be explained elsewhere.^[10] With this model, we calculate tunneling levels with energies $-2\Delta, -\Delta, \Delta, 2\Delta$ for stem rotation quantum numbers $k_{\text{stem}} = 0, \pm 1, \pm 2, 3$, respectively, as in the 1D models for hindered stem rotation only.^[1,9] The splittings $\Delta, 2\Delta, \Delta$ between consecutive levels in these quartets show the measured 1:2:1 ratio, typical for sixfold hindered rotation tunneling in the high-barrier limit. The 1D models fail to explain the experimentally observed spectrum, however, because the splittings they produce are far too small and Δ is nearly *J* independent. The coupling of stem rotation with tilt tunneling included in our model increases Δ by more than two orders of magnitude. The Coriolis coupling with the overall dimer rotation makes Δ strongly *J* dependent and, thereby, gives the difference in the splittings of the lower and upper levels involved in $\Delta J = 1$ transitions required to explain the observed line splittings (see Figure 2B). Thus, our model yields spectral line splittings in semiquantitative agreement with the measured data (see Table 1). Moreover, it predicts the experimentally observed increase of these line splittings with *J* and the smaller increase with *K*. To obtain such agreement with the measured data it is essential that the internal motion giving rise to the splittings be described as a concerted process that involves both hindered rotation of the stem and tilt tunneling. Also Coriolis coupling to the overall rotation of the complex turns out to be crucial.

Using the same theoretical approach we also investigated both mixed dimers, with C_6D_6 in the cap or with C_6D_6 in the stem. Since it is basically the sixfold hindered rotation of the stem that causes the tunneling quartets with line splittings in the ratio of 1:2:1, one would expect very similar splittings as for $(\text{C}_6\text{H}_6)_2$ when C_6D_6 is in the cap. The calculations show indeed that the quartet tunneling splittings are reduced by more than a factor of 2 when C_6D_6 is in the stem, much more than when it is in the cap. However, also with C_6D_6 in the cap it is substantial (about 25%), which is in good agreement with the 30% reduction observed experimentally (see Table V of the Supporting Information). This confirms that not only the stem hindered rotation is involved in the tunneling process but also the cap tilt motion.

After correction for microwave polarization effects, as explained in the Supporting Information, the observed intensities for the quartet lines of $(\text{C}_6\text{H}_6)_2$ show a 3:2:2:1 ratio. The lowest-frequency component of the quartet (that

Table 1: Splittings between the lines in the tunneling quartets.^[a]

$J', K' \leftarrow J, K$	Theory [kHz]			Experiment [kHz]		
5,0 \leftarrow 4,0	47.9	95.6	47.7	51.8	103.5	50.8
5,1 \leftarrow 4,1	48.1	95.9	47.8	54.4	108.9	54.7
6,2 \leftarrow 5,2	56.3	112.4	56.1	73.3	146.7	73.4
7,0 \leftarrow 6,0	62.5	124.7	62.2	73.7	146.8	74.3
7,1 \leftarrow 6,1	62.7	125.1	62.4	76.0	152.2	76.4
7,2 \leftarrow 6,2	63.2	126.2	63.0	84.0	168.6	83.5
8,1 \leftarrow 7,1	68.5	136.7	68.2	86.9	172.6	87.0
9,1 \leftarrow 8,1	73.1	146.0	72.9	97.1	195.5	97.6

[a] The splittings were calculated based on the two-dimensional cut of the *ab initio* potential^[1] used in our reduced-dimensionality model for $R = 9.42 a_0$ (the ground state vibrationally averaged intermolecular distance) and observed in the MW spectra. Only the transitions also measured for the mixed dimer are listed. For the lower tilt state the tunneling quartet levels correspond to $k_{\text{stem}} = 0, 1, 2, 3$ in increasing energy order, but their splittings decrease with increasing *J*. So the quartet of lines in the order of increasing frequencies for the $\Delta J = 1$ transitions measured corresponds to $k_{\text{stem}} = 3, 2, 1, 0$. The quartets calculated for the higher tilt states (not shown) have very similar splittings, but their frequencies increase in the order $k_{\text{stem}} = 0, 1, 2, 3$.

we can now assign to $k_{\text{stem}} = 3 \leftarrow 3$ transitions) has the highest intensity. These intensities are determined by three factors: 1) the transition line strengths, 2) the nuclear spin statistical weights of the levels involved in the transitions, and 3) the populations of the initial levels.

With regard to factor 1): Calculations with our model show that the strengths of the lines corresponding to $k_{\text{stem}} = 0, 1, 2, 3$ are very nearly equal for each quartet.

With regard to factor 2): The nuclear spin weights of different levels follow directly from the irreducible representations of the molecular symmetry (or permutation-inversion) group to which these levels belong. As shown in Ref. [1], the appropriate molecular symmetry group for the benzene dimer when cap rotation, tilt tunneling, and stem rotation tunneling are feasible, is G_{144} . Within the group G_{144} the nuclear spin statistical weights of the benzene dimer would give an intensity ratio of 1.4:1.8:2.2:1 for the tunneling quartets. Especially the relative intensities of the low-frequency tunneling components are significantly higher in the experiment.

With regard to factor 3): We know from previous investigations on molecular complexes^[11–13] that the amounts of different dimer nuclear spin species found in molecular beams are sensitive to small differences in the dissociation energies D_0 of the different dimer species (relative to the corresponding monomers). These D_0 differences play a role during dimer formation and equilibration in the expansion region of the molecular beam. This effect was studied^[8] for the mixed isotopologues of the benzene dimer: a difference in D_0 of merely about 2 cm^{-1} between $(\text{C}_6\text{D}_6)^c(\text{C}_6\text{H}_6)^s$ and $(\text{C}_6\text{H}_6)^c(\text{C}_6\text{D}_6)^s$ makes only $(\text{C}_6\text{D}_6)^c(\text{C}_6\text{H}_6)^s$ survive in the molecular beam when neon or argon is the carrier gas. Hence, it is expected that the (small) differences in D_0 for the tunneling levels of $(\text{C}_6\text{H}_6)_2$ with different k_{stem} will affect the populations of these levels in the final distribution of the dimers in the molecular beam. The dimer levels with $k_{\text{stem}} = 0, 1, 2$, and 3 are nearly isoenergetic—the internal rotation of the stem is strongly hindered and the (calculated) energy differences

between these tunneling levels are only on the order of 1 MHz—while the corresponding monomer ground state levels have rotational energies of 0, 0.28, 0.76, and 1.42 cm^{-1} , respectively. Rotation of the cap in the dimer has practically no effect on D_0 , since it remains nearly free. Therefore, the dimer levels with $k_{\text{stem}}=3$ are the most stable, with differences in D_0 relative to the $k_{\text{stem}}=0$ levels that decrease from 1.42 to 0.76 to 0.28 cm^{-1} for $k_{\text{stem}}=3, 2, 1$, respectively. Hence, the initial level populations also decrease in the order $k_{\text{stem}}=3, 2, 1, 0$. If the relative populations were given by Boltzmann factors at $T=2$ K, they would be 2.8, 1.7, 1.2, 1.0 for $k_{\text{stem}}=3, 2, 1, 0$. If we combine these populations of the levels for $k_{\text{stem}}=3, 2, 1, 0$ with the nuclear spin statistical weight ratio of 1.4:1.8:2.2:1, the experimentally observed intensity ratio of about 3:2:2:1 is rationalized.

In addition, we measured the Stark shifts of five symmetric-rotor transitions: $J+1, K \leftarrow J, K=5, 0 \leftarrow 4, 0$; $5, 1 \leftarrow 4, 1$; $7, 0 \leftarrow 6, 0$; $7, 1 \leftarrow 6, 1$; $9, 1 \leftarrow 8, 1$ of $(\text{C}_6\text{H}_6)_2$ with different electric field strengths up to 172.2 V cm^{-1} in the CAESAR arrangement.^[14] The Stark shift of a particular energy level is directly dependent on the dimer dipole moment. Consequently, the combination of Stark shift measurements with high-resolution microwave spectroscopy is well suited for the precise determination of dipole moments that will give us further important information about the dimer structure. In our measurements, we observe a linear Stark effect for $K=1$ rotational transitions, while $K=0$ transitions show a quadratic Stark effect at moderate electric field strengths. This is characteristic of a symmetric rotor. From our measurements we deduce the dipole moment of the benzene dimer $(\text{C}_6\text{H}_6)_2$, $\mu = (0.580 \pm 0.051)$ D. If we assume that the main contributions to the dipole moment of the benzene dimer are the dipole moments induced on each monomer by the electric field of the quadrupole on the other monomer site, the calculated dipole moment amounts to $\mu = 0.63$ D, in agreement with our experimental value and with an ab initio value of $\mu_{\text{calc}} = 0.51$ D for the T-shaped structure.^[15]

In summary, our measurements on $(\text{C}_6\text{H}_6)_2$ and the mixed isotopologue $(\text{C}_6\text{D}_6)^{\text{C}}(\text{C}_6\text{H}_6)^{\text{S}}$ combined with model calculations show that the tunneling process responsible for the observed quartet splittings of the rotational transitions is a concerted motion involving hindered rotation of the stem and tilt tunneling. The microwave spectra and Stark effect measurements confirm unambiguously the symmetric-rotor character observed before,^[4] which is related to the nearly free internal rotation of the benzene ring located in the cap. So, the 20-year-old mystery of the internal dynamics of the benzene dimer has been unraveled, which paves the way for further conformational and dynamical studies on aromatic molecule complexes of biological relevance.

Experimental Section

The rotational spectra of $(\text{C}_6\text{H}_6)_2$ and $(\text{C}_6\text{D}_6)^{\text{C}}(\text{C}_6\text{H}_6)^{\text{S}}$ were recorded using the high-resolution FTMW spectrometer at the Leibniz-Universität Hannover^[16] (2 to 26.5 GHz) utilizing the COBRA arrangement.^[17] The experimental setup is described in detail elsewhere.^[16,17] The spectrometer achieves line widths of about 1.5 kHz

(HWHM) for neon as the carrier gas, resulting in a resolution of about 4 kHz.

C_6H_6 and C_6D_6 were purchased from Sigma–Aldrich and used without further purification. Both are liquids at room temperature with boiling points of around 80 °C and melting points of around 6 °C. The carrier gas was flowed through a reservoir filled with pure C_6H_6 or with a 1:1 mixture of C_6H_6 and C_6D_6 followed by supersonic expansion through a pulse nozzle (General Valve Series 9) with a 0.8 mm orifice into the microwave resonator. To reduce the partial pressure of benzene, the reservoir was cooled to -15 °C with a salt–ice mixture.

Stark shift measurements of $(\text{C}_6\text{H}_6)_2$ were performed with the CAESAR setup (coaxially aligned electrodes for Stark effect applied in resonators).^[14] It provides a homogeneous electric field over the mode volume of the resonator, from which molecules are effectively contributing to the emission signal. We calibrated the field strength using the $J+1 \leftarrow J=1 \leftarrow 0$ transition of OC^{36}S (0.02 % natural abundance) using a documented dipole moment of 0.71519(3) D^[18] (see Appendix A of Ref. [19] for details).

Received: January 24, 2013

Published online: April 15, 2013

Keywords: ab initio calculations · internal rotation · noncovalent interactions · rotational spectroscopy · tunneling

- [1] A. van der Avoird, R. Podeszwa, K. Szalewicz, C. Leforestier, R. van Harrevelt, P. R. Bunker, M. Schnell, G. von Helden, G. Meijer, *Phys. Chem. Chem. Phys.* **2010**, *12*, 8219–8240.
- [2] K. C. Janda, J. C. Hemminger, J. S. Winn, S. E. Novick, S. J. Harris, W. Klemperer, *J. Chem. Phys.* **1975**, *63*, 1419–1421.
- [3] B. F. Henson, G. V. Hartland, V. A. Ventura, P. M. Felker, *J. Chem. Phys.* **1992**, *97*, 2189–2208.
- [4] E. Arunan, H. S. Gutowsky, *J. Chem. Phys.* **1993**, *98*, 4294–4296.
- [5] P. R. Bunker, P. Jensen, *Molecular Symmetry and Spectroscopy*, 2nd ed., NRC Research Press, Ottawa, Ontario, Canada, **1998**.
- [6] R. Podeszwa, R. Bukowski, K. Szalewicz, *J. Phys. Chem. A* **2006**, *110*, 10345–10354.
- [7] As explained below, this high-barrier limit applies to stem hindered rotation tunneling, which causes the observed quartet line splittings; the cap rotation is nearly free.
- [8] U. Erlekam, M. Frankowski, G. von Helden, G. Meijer, *Phys. Chem. Chem. Phys.* **2007**, *9*, 3786–3789.
- [9] V. Špirko, O. Engkvist, P. Soldan, H. L. Selzle, E. W. Schlag, *J. Chem. Phys.* **1999**, *111*, 572.
- [10] M. Schnell, U. Erlekam, P. R. Bunker, G. von Helden, J.-U. Grabow, G. Meijer, A. van der Avoird, to be published, **2013**.
- [11] A. van der Avoird, D. J. Nesbitt, *J. Chem. Phys.* **2011**, *134*, 044314.
- [12] A. van der Avoird, Y. Scribano, A. Faure, M. J. Weida, J. R. Fair, D. J. Nesbitt, *Chem. Phys.* **2012**, *399*, 28–38.
- [13] M. P. Ziemkiewicz, C. Pluetzer, D. J. Nesbitt, Y. Scribano, A. Faure, A. van der Avoird, *J. Chem. Phys.* **2012**, *137*, 084301.
- [14] M. Schnell, D. Banser, J.-U. Grabow, *Rev. Sci. Instrum.* **2004**, *75*, 2111–2115.
- [15] P. Hobza, H. L. Selzle, E. W. Schlag, *J. Chem. Phys.* **1990**, *93*, 5893–5897.
- [16] D. Banser, M. Schnell, J.-U. Grabow, E. J. Cocinero, A. Lesarri, J. L. Alonso, *Angew. Chem.* **2005**, *117*, 6469–6473; *Angew. Chem. Int. Ed.* **2005**, *44*, 6311–6315.
- [17] J.-U. Grabow, W. Stahl, H. Dreizler, *Rev. Sci. Instrum.* **1996**, *67*, 4072–4084.
- [18] J. M. L. J. Reinartz, A. Dymanus, *Chem. Phys. Lett.* **1974**, *24*, 346–351.
- [19] F. Filsinger, K. Wohlfart, M. Schnell, J.-U. Grabow, J. Küpper, *Phys. Chem. Chem. Phys.* **2008**, *10*, 666–673.